

# Probabilistic Breakdown Phenomenon at On-Ramp Bottlenecks in Three-Phase Traffic Theory

Boris S. Kerner <sup>1</sup> and Sergey L. Klenov <sup>2</sup>

<sup>1</sup> *DaimlerChrysler AG, REI/VF, HPC: T729, 70546 Stuttgart, Germany* \* and

<sup>2</sup> *Moscow Institute of Physics and Technology, Department of Physics, 141700 Dolgoprudny, Moscow Region, Russia* †

A nucleation model for the breakdown phenomenon in freeway free traffic flow at an on-ramp bottleneck is presented. This model, which can explain empirical results on the breakdown phenomenon, is based on assumptions of three-phase traffic theory in which the breakdown phenomenon is related to a first-order phase transition from the “free flow” phase to the “synchronized flow” phase. The main idea of this nucleation model is that random synchronized flow nucleation occurs within a metastable inhomogeneous steady state associated with a deterministic local perturbation in free flow, which can be considered “deterministic vehicle cluster” in free flow at the bottleneck. This deterministic vehicle cluster in free flow is motionless and exists *permanent* at the bottleneck due to the on-ramp inflow. In the nucleation model, traffic breakdown nucleation occurs through a random increase in vehicle number within this deterministic vehicle cluster, if the amplitude of the resulting random vehicle cluster exceeds some critical amplitude. The mean time delay and the associated nucleation rate of speed breakdown at the bottleneck are found and investigated. The nucleation rate of traffic breakdown as a function of the flow rates to the on-ramp and upstream of the bottleneck is studied. The nucleation model and the associated results exhibit qualitative different characteristics than those found earlier in other traffic flow nucleation models. Boundaries for speed breakdown in the diagram of congested patterns at the bottleneck are found. These boundaries are qualitatively correlated with numerical results of simulation of microscopic traffic flow models in the context of three-phase traffic theory.

PACS numbers: 89.40.+k, 47.54.+r, 64.60.Cn, 64.60.Lx

## I. INTRODUCTION

Empirical observations of freeway traffic made in various countries show that the onset of congestion in an initial free flow is associated with an abrupt decrease in vehicle speed. This speed breakdown called the “breakdown phenomenon” occurs mostly at freeway bottlenecks, in particular on-ramp bottlenecks. The speed breakdown is accompanied by a hysteresis effect (see references in the reviews [1, 2], the book [3], and the conference proceedings [4, 5, 6]). The breakdown phenomenon has a probabilistic nature [7, 8, 9]: At the same on-ramp bottleneck, speed breakdown is observed at different flow rates in different realizations (days). The probability of the breakdown is a strong increasing function of flow rate downstream of the bottleneck [8, 9].

Most mathematical theories and models of freeway traffic explain the onset of congestion in free flow by the occurrence of instability of free flow that begins at a high enough flow rate on a freeway and leads to moving jam emergence (see the reviews [10, 11, 12, 13] and the conference proceedings [14, 15, 16, 17, 18]). Consequently, at an on-ramp bottleneck moving jam(s) occurs spontaneously in free flow when the flow rate upstream of the bottleneck is high enough and the flow rate to the on-ramp increases gradually beginning from

zero [11, 12, 19, 20, 21, 22]. However, this fundamental model result that the onset of congestion in free flow is associated with spontaneous moving jam emergence [10, 11, 12, 13] is in a serious conflict with empirical evidence [3, 23, 24].

Consequently, in 1996–1999 Kerner introduced three-phase traffic theory (see [3] for a review). In this theory, there are three traffic phases: free flow, synchronized flow, and wide moving jams. In accordance with empirical investigations of phase transitions, in this theory moving jams do *not* emerge spontaneously in free flow. Rather than moving jam emergence, a phase transition from free flow to synchronized flow (F→S transition for short) governs the onset of congestion in free flow [23, 24]. A first-order F→S transition postulated in three-phase traffic theory [23] discloses the nature of the breakdown phenomenon at freeway bottlenecks found in empirical observations [1, 2]. In other words, the terms “F→S transition”, “breakdown phenomenon”, “traffic breakdown”, and “speed breakdown” are synonyms. The first microscopic models in the context of three-phase traffic theory are stochastic models [25, 26]. These models exhibit phase transitions as well as all types of congested patterns found in empirical observations [3, 25, 26, 27, 28]. Recently, some new microscopic models based on three-phase traffic theory have been developed [29, 30, 31], which can show some congested pattern features found earlier in [25, 26].

It should be noted that Mahnke et al. [34, 35] and Kühne et al. [36] have already introduced nucleation models for traffic flow that describe wide moving jam

\*Electronic address: boris.kerner@daimlerchrysler.com

†Electronic address: s-klenov@mtu-net.ru

nucleation in free flow on a homogeneous road. However, a probabilistic model description for traffic breakdown at on-ramp bottlenecks in the context of three-phase traffic theory has not been made. In this paper, a nucleation model for the probabilistic breakdown phenomenon at an on-ramp bottleneck is presented. The article is organized as follows. In Sect. II, the nucleation model is considered. Nucleation rate and the mean time delay for traffic breakdown that result from this model are studied in Sect. III. Results of the paper as well as their comparison with a nucleation model for traffic flow at an on-ramp bottleneck of Ref. [37] are discussed in Sect. IV.

## II. NUCLEATION MODEL OF TRAFFIC BREAKDOWN AT ON-RAMP BOTTLENECK

### A. Basic of nucleation model: Deterministic vehicle cluster at bottleneck

In accordance with three-phase traffic theory [3, 32], in a nucleation model we assume that the breakdown phenomenon at an on-ramp bottleneck is associated with an occurrence of a *deterministic* (permanent) local perturbation due to the on-ramp inflow. At a given high enough flow rate  $q_{in}$  in free flow on the main road upstream of the bottleneck, vehicles that merge from the on-ramp onto the main road force the vehicles on the main road to decelerate in the vicinity of an on-ramp merging region. This deceleration leads to a local decrease in speed and consequently to a local increase in density in the vicinity of the bottleneck, i.e., a local perturbation appears. In other words, the speed  $v_{free}^{(B)}$  and density  $\rho_{free}^{(B)}$  within this deterministic perturbation correspond to the conditions

$$v_{free}^{(B)} < v^{(free)}, \quad \rho_{free}^{(B)} > \rho^{(free)}, \quad (1)$$

where  $v^{(free)}$  and  $\rho^{(free)}$  are the average vehicle speed and density in homogeneous free flow on the main road downstream of the perturbation (Fig. 1 (a)). Because the on-ramp inflow occurs permanently with some rate  $q_{on}$  within the same freeway region in the vicinity of the bottleneck, the related deterministic local perturbation is also permanent and motionless. Thus, at given  $q_{in}$  and  $q_{on}$ , the total flow rate does not depend on the spatial co-ordinate, i.e., the speed and density on the main road satisfy the following condition:

$$q_{sum} = v^{(free)} \rho^{(free)} = v_{free}^{(B)} \rho_{free}^{(B)}, \quad (2)$$

where

$$q_{sum} = q_{in} + q_{on}. \quad (3)$$

The inhomogeneous steady state within the deterministic local perturbation can be considered “deterministic vehicle cluster” in free flow localized at the bottleneck or “deterministic cluster” for short. This deterministic

vehicle cluster in free flow is motionless and exists permanent at the bottleneck due to the on-ramp inflow.

When  $q_{on}$  is a given value and the total flow rate  $q_{sum}$  increases, then the vehicle speed  $v_{free}^{(B)}$  within the deterministic cluster decreases and in accordance with (2) the associated density  $\rho_{free}^{(B)}$  increases. However, this increase is limited by some critical density  $\rho_{free}^{(B)} = \rho_{determ, FS}^{(B)}$  (Fig. 1 (c)) within the deterministic cluster associated with a critical flow rate

$$q_{sum} = q_{determ, FS}^{(B)}. \quad (4)$$

After this critical deterministic perturbation is reached, the further increase in  $q_{sum}$  leads to *deterministic traffic breakdown* at the bottleneck causing spontaneous synchronized flow emergence at the bottleneck. The critical deterministic perturbation can be considered “critical deterministic vehicle cluster” (“critical deterministic cluster” for short) or “deterministic nuclei for speed breakdown”. After the critical deterministic cluster is reached, deterministic traffic breakdown occurs at the bottleneck even if there are no random perturbations in traffic flow at the bottleneck.

Random perturbations within the initial deterministic cluster can cause random speed breakdown (F→S transition) at the flow rate

$$q_{sum} < q_{determ, FS}^{(B)}, \quad (5)$$

i.e., before the deterministic nuclei for speed breakdown is reached. In this case, random traffic breakdown nucleation can occur at the bottleneck (arrows labeled F→S in Fig. 1 (b, c)). This is realized, if through a random increase in vehicle number within the initial deterministic cluster, the amplitude of the resulting “random vehicle cluster” (“random cluster” for short) exceeds some critical amplitude associated with a critical density within the random cluster  $\rho_{cr, FS}^{(B)}$  (Fig. 1 (c)). The random cluster with the critical density  $\rho_{cr, FS}^{(B)}$  can be considered “critical random vehicle cluster” at the bottleneck (“critical random cluster” for short) or “random nuclei for speed breakdown”. If the amplitude of a random cluster is smaller than the critical one, the random cluster decays towards the initial deterministic cluster.

Speed states within the deterministic cluster  $v_{free}^{(B)}(q_{sum})$ , the speed within the critical random cluster  $v_{cr, FS}^{(B)}(q_{sum})$ , along with a 2D synchronized flow speed states [3], together form a Z-shaped speed-flow characteristic for speed breakdown (Fig. 1 (b)). The associated density-flow characteristic (Fig. 1 (b)), which consists of density states within the deterministic cluster  $\rho_{free}^{(B)}(q_{sum})$ , the density within the critical random cluster  $\rho_{cr, FS}^{(B)}(q_{sum})$ , along with a 2D synchronized flow states, has obviously a S-shaped form (Fig. 1 (c)). Due to an F→S transition, precipitous cluster growth at the bottleneck occurs leading to congested pattern formation, i.e., either a synchronized flow pattern (SP)

or a general pattern (GP) appears upstream of the bottleneck [3]. However, the nucleation effect leading to traffic breakdown and its characteristics are fully independent of possible congested patterns resulting from this F→S transition. For this reason, we can average the infinity of synchronized flow states (dashed regions in (b, c)) for each given flow rate  $q_{\text{sum}}$  to one speed  $v_{\text{syn, aver}}^{(B)}(q_{\text{sum}})$  and to one density  $\rho_{\text{syn, aver}}^{(B)}(q_{\text{sum}})$  (Fig. 1 (d, e)) [33]. A consideration of the resulting congested patterns is beyond the scope of this article.

### B. Master equation

We consider the dynamics of the total vehicle number  $N$  within the vehicle cluster localized at the bottleneck (dashed region in Fig. 1 (a)). It is assumed that downstream and upstream of the cluster homogeneous free traffic flows occur. The total number of vehicles  $N$  within the cluster can either increase or decrease over time randomly in comparison with a value  $N = N^{(\text{determ})}$  for the case in which the deterministic cluster exists at the bottleneck only.

As in other nucleation models for traffic flow first introduced by Mahnke et al. [34, 35], for a description of random cluster evolution we use a master equation. The probability  $p(N, t)$  to find  $N$  vehicles within the cluster at the bottleneck reads as follows

$$\frac{\partial p(N, t)}{\partial t} = w_+(N-1)p(N-1, t) + w_-(N+1)p(N+1, t) - [w_+(N) + w_-(N)]p(N, t), \quad \text{at } N > 0, \quad (6)$$

$$\frac{\partial p(0, t)}{\partial t} = w_-(1)p(1, t) - w_+(0)p(0, t), \quad \text{at } N = 0, \quad (7)$$

with the boundary condition

$$w_-(0) = 0, \quad (8)$$

where  $w_+$  is the vehicle attachment rate onto the cluster and  $w_-$  is the vehicle detachment rate from the cluster. In the model, the vehicle attachment rate  $w_+$  is independent of  $N$ , i.e.,

$$w_+ = q_{\text{sum}}. \quad (9)$$

### C. Vehicle detachment rate from cluster

The vehicle detachment rate  $w_-$  is obviously equal to the outflow rate from the cluster

$$w_-(N) = q_{\text{down}}^{(\text{bottle})}(N). \quad (10)$$

In the model, it is assumed that the shape of the characteristic  $q_{\text{down}}^{(\text{bottle})}(N)$  (Fig. 2) follows from the S-shaped

density–flow characteristic of three-phase traffic theory (Fig. 1 (e)): The characteristic  $q_{\text{down}}^{(\text{bottle})}(N)$  has at least two different branches  $q_{\text{down}}^{(\text{bottle})}(N)$  labeled  $N^{(\text{determ})}$  and  $N_c$  in Fig. 2 (a). These branches are related to the vehicle number ranges, respectively, given by the conditions

$$0 \leq N \leq N_d \quad (11)$$

and

$$N_d < N \leq N_s. \quad (12)$$

The branches  $N^{(\text{determ})}$  and  $N_c$  in Fig. 2 (a) are associated with the density branches  $\rho_{\text{free}}^{(B)}$  and  $\rho_{\text{cr, FS}}^{(B)}$  of the S-shaped density–flow characteristic in Fig. 1 (e), respectively. The branch  $N^{(\text{determ})}$  is associated with the case in which at a high enough flow rate  $q_{\text{sum}}$  and the on-ramp flow rate  $q_{\text{on}} > 0$  the deterministic cluster exists at the bottleneck. The branch  $N_c$  is associated with the case in which the critical random cluster whose growth leads to an F→S transition occurs at the bottleneck.

In addition, from the S-shaped density–flow characteristic (Fig. 1 (e)) can be seen that for the case in which an LSP results from an F→S transition [33], at

$$N > N_s, \quad (13)$$

there is a third branch  $N^{(\text{syn})}$  on the characteristic  $q_{\text{down}}^{(\text{bottle})}(N)$  (Fig. 2 (a)) associated with the branch  $\rho_{\text{syn, aver}}^{(B)}$  for averaged synchronized flow states in Fig. 1 (e). In this case,  $q_{\text{down}}^{(\text{bottle})}(N)$  (10) is a N-shaped flow–vehicle-number characteristic.

At the critical point  $N = N_d$  at which the branches  $N^{(\text{determ})}$  and  $N_c$  merges, the function  $q_{\text{down}}^{(\text{bottle})}(N)$  has its maximum point. At the threshold point  $N = N_s$  at which the branches  $N_c$  and  $N^{(\text{syn})}$  merges, the function  $q_{\text{down}}^{(\text{bottle})}(N)$  has its minimum point. Quantitative characteristics of the N-shaped function  $q_{\text{down}}^{(\text{bottle})}(N)$  (e.g., values  $N_d$  and  $N_s$ ) can depend on the flow rate to the on-ramp  $q_{\text{on}}$ : It can turn out that at the same  $N$  the greater  $q_{\text{on}}$ , the more difficult for vehicles to escape from the cluster, i.e., the less  $q_{\text{down}}^{(\text{bottle})}$  is. This possible case that is confirmed by microscopic simulations [26] is reflected in Fig. 2 (b) in which it is assumed that the greater  $q_{\text{on}}$ , the greater  $N_d$  and  $N_s$  are. Thus, in a general case instead of (10) we should use

$$w_-(N) = q_{\text{down}}^{(\text{bottle})}(N, q_{\text{on}}). \quad (14)$$

A possible impact of the flow rate  $q_{\text{on}}$  on quantitative characteristics of the mean time delay for an F→S transition is discussed in Sect. IV.

### D. Steady states

Steady states of vehicle number  $N$  at given  $q_{\text{in}}$  and  $q_{\text{on}}$  are associated with solutions of the equation

$$w_+ = w_-(N). \quad (15)$$

In accordance with (9), (14), they are found from the condition

$$q_{\text{sum}} = q_{\text{down}}^{(\text{bottle})}(N, q_{\text{on}}). \quad (16)$$

As can be seen from Fig. 2 (a), at given flow rates  $q_{\text{on}}$  and  $q_{\text{in}}$  that satisfy the condition

$$q_{\text{th}}^{(\text{B})} < q_{\text{sum}} < q_{\text{determ, FS}}^{(\text{B})} \quad (17)$$

there can be at least two steady states:  $N = N_1$  associated with the deterministic cluster and  $N = N_2$  associated with the critical random cluster. These steady states are the roots of Eq. (16), i.e., they are associated with the intersection points of the horizontal line  $q_{\text{down}}^{(\text{bottle})} = q_{\text{sum}}$  with the branches  $N^{(\text{determ})}$  and  $N_c$  of the characteristic  $q_{\text{down}}^{(\text{bottle})}(N, q_{\text{on}})$  (Fig. 2 (a)), respectively. In addition, if an LSP occurs as a result of an F→S transition [33], then there is a third root of Eq. (16),  $N = N_3$ , associated with the intersection point of the horizontal line  $q_{\text{down}}^{(\text{bottle})} = q_{\text{sum}}$  with the branch  $N^{(\text{syn})}$  of the characteristic  $q_{\text{down}}^{(\text{bottle})}(N)$ .

If the flow rate  $q_{\text{sum}}$  increases, then the critical vehicle number difference within the cluster

$$\Delta N_c = N_2 - N_1 \quad (18)$$

decreases. This critical vehicle number difference is associated with the vehicle number difference within the critical random cluster and within the initial deterministic cluster at the bottleneck. The growth of the critical random cluster leads to traffic breakdown at the bottleneck.

At the critical flow rate (4), we get  $\Delta N_c = 0$ : The steady states  $N_1$  and  $N_2$  merge into one point with the critical vehicle number  $N = N_d$  at which  $q_{\text{determ, FS}}^{(\text{B})} = q_{\text{down}}^{(\text{bottle})}(N_d, q_{\text{on}})$ . At  $q_{\text{sum}} \geq q_{\text{determ, FS}}^{(\text{B})}$  the deterministic speed breakdown should occur even if there is no random increase in the vehicle number within the initial deterministic cluster at the bottleneck.

If the flow rate  $q_{\text{sum}}$  decreases gradually, then the threshold flow rate

$$q_{\text{sum}} = q_{\text{th}}^{(\text{B})} \quad (19)$$

is reached at which the steady states  $N_2$  and  $N_3$  merge into one threshold steady state  $N = N_s$  at which  $q_{\text{th}}^{(\text{B})} = q_{\text{down}}^{(\text{bottle})}(N_s, q_{\text{on}})$ .

### III. NUCLEATION RATE OF SPEED BREAKDOWN AT BOTTLENECK

As follows from the analysis of the model (6)-(9), (14) (Appendix A), in the flow range (17) the mean time delay of an F→S transition at the bottleneck is

$$T_{\text{FS}}^{(\text{B, mean})} = C \exp \{ \Delta \Phi \}, \quad (20)$$

where a potential barrier

$$\Delta \Phi = \Phi(N_2) - \Phi(N_1), \quad (21)$$

the potential  $\Phi(N)$  is

$$\Phi(N) = \begin{cases} \sum_{n=1}^N \ln \frac{w_-(n)}{w_+} & \text{at } N > 0, \\ 0 & \text{at } N = 0, \end{cases} \quad (22)$$

$$C = 2\pi \left( w'_-(N_1) \mid w'_-(N_2) \mid \right)^{-\frac{1}{2}}, \quad (23)$$

$w'_-(N) = dw_-/dN$ . Respectively, the nucleation rate for speed breakdown at the bottleneck is

$$G_{\text{FS}}^{(\text{B})} = \frac{1}{T_{\text{FS}}^{(\text{B, mean})}} = C^{-1} \exp \{ -\Delta \Phi \}. \quad (24)$$

To find a qualitative shape  $\Phi(N)$  (22) (Fig. 3), a change in  $\Phi(N)$  between two neighboring points  $N$  and  $N - 1$  that equals

$$\delta \Phi(N) = \Phi(N) - \Phi(N - 1) = \ln \frac{w_-(N)}{w_+} \quad (25)$$

can be used. The value  $\delta \Phi(N)$  (25) becomes zero at the maximum and minimum points of the function  $\Phi(N)$ , i.e., at the roots of Eq. (15) that are the points  $N = N_i$ ,  $i = 1, 2, 3$  discussed above (Fig. 2 (a)). The value  $\delta \Phi(N) > 0$  at  $w_-(N) > w_+$ , i.e., at points of the curve  $w_-(N)$  above the horizontal line  $q = q_{\text{sum}}$  in (Fig. 2 (a)). In contrast,  $\delta \Phi(N) < 0$  at  $w_-(N) < w_+$ , i.e., at points of the curve  $w_-(N)$  below the horizontal line  $q = q_{\text{sum}}$ .

It can be seen from (20) that the mean time delay for speed breakdown decreases exponentially with increase in potential barrier  $\Delta \Phi$  (21). If in Fig. 3 the total flow rate increases from  $q_{\text{sum}} = q_{\text{sum}}^{(1)}$  to  $q_{\text{sum}} = q_{\text{sum}}^{(2)}$ , which is close to the critical flow rate (4) for deterministic speed breakdown, then the potential barrier  $\Delta \Phi$  (21) decreases from  $\Delta \Phi_1$  to  $\Delta \Phi_2$ .

In contrast, if the total flow rate decreases from  $q_{\text{sum}} = q_{\text{sum}}^{(1)}$  to  $q_{\text{sum}} = q_{\text{sum}}^{(3)}$ , which is close to the threshold flow rate  $q_{\text{th}}^{(\text{B})}$  (19) for random speed breakdown, then the potential barrier  $\Delta \Phi$  (21) increases from  $\Delta \Phi_1$  to  $\Delta \Phi_3$  (Fig. 3). At the threshold point  $q_{\text{sum}} = q_{\text{th}}^{(\text{B})}$  (19), the potential barrier  $\Delta \Phi(N)$  reaches the maximum value

$$\Delta \Phi = \Phi(N_s) - \Phi(N_{\text{th}}), \quad (26)$$

where  $N_{\text{th}} = N_1$  at  $q_{\text{sum}} = q_{\text{th}}^{(\text{B})}$ . As a result, the mean time delay  $T_{\text{FS}}^{(\text{B, mean})}$  (20) strongly increases as  $q_{\text{sum}}$  approaches the threshold point  $q_{\text{th}}^{(\text{B})}$ . Under the condition

$$q_{\text{sum}} < q_{\text{th}}^{(\text{B})} \quad (27)$$

no speed breakdown at the bottleneck regardless of a random increase in the vehicle number within the cluster is possible at the bottleneck.

If in the vicinity of the critical vehicle number  $N_d$  the potential  $\Phi(N)$  (Fig. 3) can be approximated by a parabolic function of  $N$ , then the following approximate formula can be derived from (20) (Appendix A):

$$T_{\text{FS}}^{(\text{B, mean})} = \frac{\sqrt{2}\pi N_d}{q_{\text{determ, FS}}^{(\text{B})} (\xi_d \Delta_c)^{1/2}} \exp\left(\frac{8N_d \Delta_c^{3/2}}{3\sqrt{2}\xi_d}\right), \quad (28)$$

where

$$\xi_d = -(N^2 d^2 \ln w_- / dN^2)|_{N=N_d} \quad (29)$$

is a dimensionless value of the order of 1,

$$\Delta_c = \frac{q_{\text{determ, FS}}^{(\text{B})} - q_{\text{sum}}}{q_{\text{determ, FS}}^{(\text{B})}}, \quad (30)$$

i.e.,  $\Delta_c$  is the relative difference between the critical flow rate  $q_{\text{determ, FS}}^{(\text{B})}$  for the deterministic F→S transition and the total flow rate  $q_{\text{sum}}$  (3). Respectively, the nucleation rate  $G_{\text{FS}}^{(\text{B})} = 1/T_{\text{FS}}^{(\text{B, mean})}$  for speed breakdown at the bottleneck is

$$G_{\text{FS}}^{(\text{B})} = \frac{q_{\text{determ, FS}}^{(\text{B})} (\xi_d \Delta_c)^{1/2}}{\sqrt{2}\pi N_d} \exp\left(-\frac{8N_d \Delta_c^{3/2}}{3\sqrt{2}\xi_d}\right). \quad (31)$$

Note that  $q_{\text{determ, FS}}^{(\text{B})}$ ,  $N_d$ , and  $\xi_d$  depend  $q_{\text{on}}$ . Therefore, the mean time delay  $T_{\text{FS}}^{(\text{B, mean})}$  (28) and the nucleation rate  $G_{\text{FS}}^{(\text{B})}$  (31) are functions of  $q_{\text{sum}}$  and  $q_{\text{on}}$ .

If the flow rate  $q_{\text{on}}$  decreases continuously up to a small enough value (however, we assume that  $q_{\text{on}} > 0$ , i.e., the deterministic cluster still exists at the bottleneck), then the values  $\xi_d$ ,  $N_d$ , and  $q_{\text{determ, FS}}^{(\text{B})}$  in (30), (31) and, therefore, the nucleation rate  $G_{\text{FS}}^{(\text{B})}$  (31) do *not* decrease proportionally to this decrease in  $q_{\text{on}}$ . In contrast, in this limit case  $\xi_d \rightarrow \xi_{d, \text{lim}}$ ,  $N_d \rightarrow N_{d, \text{lim}}$ , and  $q_{\text{determ, FS}}^{(\text{B})} \rightarrow q_{\text{determ, lim}}^{(\text{B})}$ , where  $\xi_{d, \text{lim}}$ ,  $N_{d, \text{lim}}$ , and  $q_{\text{determ, lim}}^{(\text{B})}$  are constants. Taking into account that in this case in  $\Delta_c$  (30) the flow rate  $q_{\text{determ, FS}}^{(\text{B})} \approx q_{\text{determ, lim}}^{(\text{B})} = \text{const}$ , we can see that at small enough values of  $q_{\text{on}}$  the nucleation rate for speed breakdown (31) depends on the total flow rate  $q_{\text{sum}}$  only. In other words, in this limit case at a given  $q_{\text{sum}}$  within the flow range (17) the nucleation rate for traffic breakdown at the bottleneck (31) tends to a finite constant value, which is greater than zero (see Sect. IV).

When  $q_{\text{on}} = 0$ , the road can be considered homogeneous one without bottlenecks. Then there is no deterministic perturbation (deterministic cluster) at the bottleneck and, therefore, the nucleation model and results of this article cannot be applied. In three-phase traffic theory, the breakdown phenomenon can also occur in this case. However, at the same conditions, in particular, the same flow rates downstream of the bottleneck and on a homogeneous road, the nucleation rate for speed breakdown on the homogeneous road is considerably smaller

than at the bottleneck [3, 27]. This is associated with empirical results in which the breakdown phenomenon has also been observed away from bottlenecks, however, this speed breakdown is much more rare than at an on-ramp bottleneck [3]. A consideration of a nucleation model of the breakdown phenomenon for a homogeneous road is beyond the scope of this article.

As usual for each first-order phase transition observed in many other systems in natural science [38], the nucleation rate for speed breakdown (31) is an exponential function of  $\Delta_c$  (30). For traffic flow, in accordance with (31) and (30) the exponential growth of the nucleation rate with  $\Delta_c$  (30) is very sensible to the critical value for the deterministic breakdown phenomenon  $q_{\text{determ, FS}}^{(\text{B})}$ . This emphasize the important impact of the deterministic cluster, which occurs at the bottleneck at  $q_{\text{on}} > 0$ , on the nucleation rate for speed breakdown (31) at a given total flow rate  $q_{\text{sum}}$ .

#### IV. DISCUSSION

Let us compare general results of the nucleation model presented in Sect. III with the diagram of congested patterns at an on-ramp bottleneck postulated in [24] and found in numerical simulations of microscopic traffic flow models [25, 26], as well as with a microscopic theory of the breakdown phenomenon [27]. To reach this goal, we consider an example of the function  $w_-$  (14)

$$w_-(N) = N \left[ \frac{a}{1 + (N/N_0)^4} + b \right], \quad (32)$$

where  $a$ ,  $b$ , and  $N_0$  are functions of  $q_{\text{on}}$ :  $a(q_{\text{on}}) = 1.32q_0(q_{\text{on}})/N_0(q_{\text{on}})$  1/h,  $q_0(q_{\text{on}}) = 2700 - 370(1 + q_{\text{on}}/300)^{-1}$  vehicles/h,  $b(q_{\text{on}}) = 33 - 10(1 + q_{\text{on}}/250)^{-1}$  1/h,  $N_0(q_{\text{on}}) = 25 + 6.5(1 + q_{\text{on}}/300)^{-1}$  vehicles. The analytical function (32) allows us to perform a numerical analysis of the mean time delay (20) and the associated nucleation rate (24) for the breakdown phenomenon. As in the general model (Fig. 2), the function (32) is a N-shape flow–vehicle-number characteristic (Fig. 4 (a)) and the potential  $\Phi$  shows qualitatively the same behavior at different total flow rates  $q_{\text{sum}}$  (Fig. 4 (b)) as those in Fig. 3.

The potential barrier  $\Delta\Phi$  in (20), (24) (Fig. 5 (a)) and the associated critical vehicle number difference  $\Delta N_c$  (18) are decreasing functions of the total flow rate  $q_{\text{sum}}$ ; at a given  $q_{\text{sum}}$  they can also be decreasing functions of  $q_{\text{on}}$  (Fig. 5 (b)). For these reasons, the total flow rate dependences of the mean time delay  $T_{\text{FS}}^{(\text{B, mean})}$  (20) (Fig. 5 (c, d)) and of the associated nucleation rate for speed breakdown at the bottleneck (Fig. 5 (e, f)) exhibit qualitative features observed in traffic flow at on-ramp bottlenecks [8, 9] and found in a microscopic three-phase traffic theory [26, 27]. This confirms that the breakdown phenomenon at the bottleneck is a first-order F→S transition [3]. In all these curves, the total flow rate  $q_{\text{sum}}$

is smaller than the critical flow rate for the deterministic speed breakdown  $q_{\text{determ, FS}}^{(B)}$  (4). This means that  $\Delta_c$  (30) is not equal zero for all results in Fig. 5, i.e., speed breakdown occurs due to a random density increase within an initial deterministic cluster at the bottleneck. The total flow rate dependences of the nucleation rate for speed breakdown  $G_{\text{FS}}^{(B)}$  (24) calculated at different flow rates  $q_{\text{on}}$  exhibit features of three-phase traffic theory in which the breakdown phenomenon can also occur at small values  $q_{\text{on}}$ .

The critical boundary  $F_{S, \zeta}^{(B)}$  (Fig. 6 (a, b)) in the diagram of congested patterns at the bottleneck (flow-flow plane with the coordinates  $(q_{\text{on}}, q_{\text{in}})$ ) is associated with the cases in which the nucleation rate for speed breakdown is a given value  $\zeta$ . Therefore, the boundary  $F_{S, \zeta}^{(B)}$  satisfies the condition

$$G_{\text{FS}}^{(B)}(q_{\text{sum}}, q_{\text{on}}) = \zeta, \quad \zeta = \text{const}, \quad (33)$$

i.e., at the boundary  $F_{S, \zeta}^{(B)}$  the flow rate

$$q_{\text{sum}} = q_G^{(B)}(q_{\text{on}}) \quad (34)$$

depends on  $q_{\text{on}}$ . This boundary is qualitatively similar with the critical boundary  $F_S^{(B)}$  in the diagram at which the probability for speed breakdown for a given time  $T_{\text{ob}}$  for observing traffic flow is 1 [3]. In the diagram, there is also the threshold boundary  $F_{\text{th}}^{(B)}$  (curve  $F_{\text{th}}^{(B)}$  in Fig. 6 (b)) at which the condition (19) is satisfied. The threshold boundary also exhibits the same qualitative features as those found in simulation of phase transitions and spatiotemporal congested patterns in a microscopic three-phase traffic theory [3, 27]. In particular, in the limiting case of small values  $q_{\text{on}}$  (but  $q_{\text{on}} > 0$ , i.e., it is assumed that the deterministic cluster still exists at the bottleneck) the flow rate  $q_G^{(B)}$  reaches the maximum (limit) value  $q_{G, \text{lim}}^{(B)}$  at a given nucleation rate for speed breakdown  $\zeta$  (33).

The greater the nucleation rate for speed breakdown, the greater  $q_{G, \text{lim}}^{(B)}$  should be. However, the increase in nucleation rate for speed breakdown has a limit associated with deterministic speed breakdown occurrence: When  $\zeta$  in (33) increases, the boundary  $F_{S, \zeta}^{(B)}$  for random speed breakdown tends to the boundary  $F_{\text{determ, S}}^{(B)}$  (curves  $F_{\text{determ, S}}^{(B)}$  in Fig. 6 (a, b)) for deterministic speed breakdown in the diagram of congested patterns. At the boundary  $F_{\text{determ, S}}^{(B)}$ , the deterministic breakdown phenomenon occurs within the deterministic cluster even if *no* random vehicle number increase within the deterministic cluster appears at the bottleneck. When  $\zeta$  in (33) decreases, the boundary  $F_{S, \zeta}^{(B)}$  tends to the threshold boundary  $F_{\text{th}}^{(B)}$  (curve  $F_{\text{th}}^{(B)}$  in Fig. 6 (b)). In accordance with a microscopic theory [27], in the nucleation model the flow rate  $q_G^{(B)}$  (34) (curves 1–4 in Fig. 6 (c, d)), the critical flow rate  $q_{\text{determ, FS}}^{(B)}$  for deterministic speed breakdown

(curves  $q_{\text{determ, FS}}^{(B)}$  in Fig. 6 (c, d)), as well as the threshold flow rate  $q_{\text{th}}^{(B)}$  (19) (curve  $q_{\text{th}}^{(B)}$  in Fig. 6 (d)) can be the smaller, the greater  $q_{\text{on}}$  is.

To compare the results of our nucleation model with a nucleation model for the breakdown phenomenon at the on-ramp bottleneck introduced by Kühne et al. [37], it should be noted that in [37], even if the on-ramp inflow rate  $q_{\text{on}}$  is high, in an initial steady state of traffic flow there is no deterministic cluster at the bottleneck. As a result, there is no deterministic breakdown phenomenon of three-phase traffic theory in this model.

Probably for this reason, in the model [37] the nucleation rate for the breakdown phenomenon (generation rate of speed breakdown critical nuclei) is proportional to the on-ramp inflow rate  $q_{\text{on}}$ . As a result, if  $q_{\text{on}}$  decreases below a small enough value (but  $q_{\text{on}} > 0$ ) and the total flow rate  $q_{\text{sum}}$  increases (through an increase in  $q_{\text{in}}$ ), a reasonable given nucleation rate for traffic breakdown at the bottleneck (the nucleation rate should be greater than  $\approx 1/20 \text{ min}^{-1}$ , in accordance with empirical observations [8, 9]) cannot be reached. This is true in the nucleation model of [37] even if the total flow rate is equal to a critical value associated with the critical nuclei for speed breakdown consisting of *one vehicle* only (in [37] this critical value is denoted by  $q_{c2}$ ).

In contrast, in our model the nucleation rate (generation rate of critical nuclei) for the breakdown phenomenon is *not* proportional to  $q_{\text{on}}$  and, therefore, as mentioned in Sect. III, for the limiting case of small values  $q_{\text{on}}$  (however, we assume that  $q_{\text{on}} > 0$ , specifically, the deterministic cluster still exists at the bottleneck) this generation rate of critical nuclei depends on the total flow rate  $q_{\text{sum}}$  *only*, i.e., this generation rate does *not* depend on  $q_{\text{on}}$ . At a given  $q_{\text{sum}}$ , an increase in  $q_{\text{on}}$  can influence *only* on such characteristics of speed breakdown as the critical flow rate  $q_{\text{determ, FS}}^{(B)}$  and the threshold flow rate  $q_{\text{th}}^{(B)}$ , as well as on congested traffic states at the bottleneck that result from the breakdown phenomenon.

When  $q_{\text{sum}}$  increases, the nucleation rate of traffic breakdown increases in the both models. However, in our model the nucleation rate cannot exceed the nucleation rate for traffic breakdown associated with the deterministic breakdown phenomenon. In contrast with assumptions of the nucleation model of Ref. [37], the deterministic traffic breakdown occurs even *without* any random vehicle number increase within the initial steady state of free flow at the bottleneck. This is because if  $q_{\text{on}} > 0$ , then in our model there is a deterministic vehicle cluster localized at the bottleneck, which exists permanent at the bottleneck due to the on-ramp inflow. In our model, random traffic breakdown nucleation can occurs through a random increase in vehicle number *within this deterministic cluster*. The mentioned qualitative differences in the nucleation model of Ref. [37] and our nucleation model are also responsible for different dependences of the generation rate of traffic breakdown on the total flow rate in these nucleation models.

## APPENDIX A

In order to derive formula (20), we use a general formula for the mean time delay  $T$  of escaping from the potential well for the master equation (6) [38]:

$$T = \sum_{n=N_1}^{N_3} \left[ (w_+ p_s(n))^{-1} \sum_{k=0}^n p_s(k) \right], \quad (\text{A1})$$

where  $p_s(N)$  is a steady solution of (6), (7):

$$p_s(N) = p_s(0) \prod_{n=1}^N \frac{w_+}{w_-(n)} \quad \text{at } N > 0. \quad (\text{A2})$$

When  $N_i \gg 1$ ,  $i = 1, 2$  (more rigorous conditions are given below), the distribution  $p_s(N)$  has a sharp maximum at  $N = N_1$ , and the function  $p_s^{-1}(n)$  in (A1) has a sharp maximum at  $n = N_2$ . Then the formula (A1) can be written as follows [38]:

$$T = (w_+)^{-1} \sum_{n=0}^{N_2} p_s(n) \sum_{n=N_1}^{N_3} p_s^{-1}(n). \quad (\text{A3})$$

Formula (A2) can be written as [36]

$$p_s(N) = p_s(0) \exp[-\Phi(N)] \quad \text{at } N \geq 0, \quad (\text{A4})$$

where the potential  $\Phi(N)$  is given by (22). Substituting (A4) into (A3), we can find the exponentially large factor in (A3) explicitly

$$T = (w_+)^{-1} c_1 c_2 \exp[\Phi(N_2) - \Phi(N_1)], \quad (\text{A5})$$

where

$$c_1 = \sum_{n=0}^{N_2} \exp[-\Delta\Phi^{(1)}(n)], \quad c_2 = \sum_{n=N_1}^{N_3} \exp[\Delta\Phi^{(2)}(n)], \quad (\text{A6})$$

$$\Delta\Phi^{(i)}(N) = \Phi(N) - \Phi(N_i), \quad i = 1, 2. \quad (\text{A7})$$

The factors  $c_1$ ,  $c_2$  can be estimated using the parabolic approximation of potential  $\Phi(N)$  near the extremum points  $N = N_1$ ,  $N_2$  [39]. For instance, to find the factor  $c_1$ , we introduce a new variable  $y = N/N_1$  and approximate the sums in (22), (A6) by integrals:

$$\Delta\Phi^{(1)}(N) \approx \phi^{(1)}(y) = N_1 \int_1^y \ln \frac{w_-(N_1 z)}{w_+} dz, \quad (\text{A8})$$

$$c_1 \approx N_1 \int_0^{N_2/N_1} \exp[-\phi^{(1)}(y)] dy. \quad (\text{A9})$$

Using the series expansion

$$\phi^{(1)}(y) = N_1 \eta_1 (y-1)^2/2 + O((y-1)^3) \quad (\text{A10})$$

near the point  $y = 1$ , where  $\eta_1 = d \ln w_- / d \ln N|_{N=N_1}$ , we find  $c_1 = \sqrt{2\pi N_1/\eta_1}$ . Similarly,  $c_2 = \sqrt{2\pi N_2/\eta_2}$ , where  $\eta_2 = -d \ln w_- / d \ln N|_{N=N_2}$ . The substitution of  $c_1$  and  $c_2$  into (A5) yields the formula (20).

The parabolic approximation used for estimation of factor  $c_1$  holds only when we can neglect in integral (A9) third-order terms in the potential expansion (A10) [39]. The same is true for calculation of  $c_2$ . The conditions of the parabolic approximation are

$$N_i \eta_i^3 \gtrsim \xi_i^2, \quad i = 1, 2, \quad (\text{A11})$$

where  $\xi_i = N_i^2 d^2 \ln w_- / dN^2|_{N=N_i}$ ,  $i = 1, 2$ .

To derive the formula (28), we approximate the value  $\Delta\Phi$  in (20) by integral

$$\Delta\Phi = N_1 \int_1^{N_2/N_1} \ln \frac{w_-(N_1 y)}{w_+} dy. \quad (\text{A12})$$

Under the condition that  $q_{\text{sum}}$  is close to the critical point  $q_{\text{determin, FS}}^{(B)}$ , i.e., when

$$\Delta_c \ll 1, \quad (\text{A13})$$

we can approximate the function  $w_-(N)$  in (A12) near the maximum point  $N = N_d$  by parabola:

$$w_-(N) = q_{\text{determin, FS}}^{(B)} \left[ 1 - \xi_d \frac{(N - N_d)^2}{2N_d^2} \right], \quad (\text{A14})$$

where the formula  $q_{\text{determin, FS}}^{(B)} = w_-(N_d)$  is taken into account. Under the condition (A13), roots  $N = N_1$  and  $N = N_2$  of equation  $q_{\text{sum}} = w_-(N)$  given by formulae (14), (16) are close to the critical point  $N = N_d$ . Then from (14), (16), (A14) we can estimate  $N_1$  and  $N_2$  as

$$N_{1,2} = N_d \mp \Delta N_c/2, \quad (\text{A15})$$

where the critical value  $\Delta N_c$  (18) is

$$\Delta N_c = 2\sqrt{2}\xi_d^{-1/2} N_d \Delta_c^{1/2}. \quad (\text{A16})$$

Substituting (A14)–(A16) into (A12) and integrating (A12), we find

$$\Delta\Phi = \frac{8N_d \Delta_c^{3/2}}{3\sqrt{2}\xi_d}. \quad (\text{A17})$$

Using (A14) and (A15), we can also estimate the derivatives  $w'_-(N_i)$  in (23):  $w'_-(N_i) \approx \pm q_{\text{determin, FS}}^{(B)} \xi_d \Delta N_c / (2N_d^2)$ ,  $i = 1, 2$ . Then the substitution of the latter formula together with (A16), (A17) into (20) leads to formula (28).

Note that the approximate formula (28) is applicable under the condition (A13) only if the conditions (A11) are still satisfied. Using the above formula for derivatives  $w'_-(N_i)$ ,  $i = 1, 2$  and that  $N_i$ ,  $i = 1, 2$  is close to  $N_d$ , we can estimate the values  $\xi_i \approx \xi_d$  and  $\eta_i \approx \xi_d \Delta N_c / N_d$ ,  $i = 1, 2$  in (A11). Thus, the condition

(A11) reads  $\xi_d \Delta N_c^3 / N_d^2 \gtrsim 1$ . Taking into account formula (A16) for  $\Delta N_c$ , the condition (A11) can be written in terms of  $\Delta_c$ :

$$N_d \Delta_c^{3/2} \xi_d^{-1/2} \gtrsim 1. \quad (\text{A18})$$

This inequality together with (A13) determine the range of  $\Delta_c$  in which the approximate formula (28) for the mean time delay  $T_{\text{FS}}^{(\text{B}, \text{mean})}$  of an F→S transition at the bottleneck is valid.

- 
- [1] F.L. Hall, V.F. Hurdle, J.H. Banks, *Transportation Research Record* **1365**, 12–18 (1992).
  - [2] J.H. Banks, *Transportation Research Record* **1802**, 225–232 (2002).
  - [3] B.S. Kerner. *The Physics of Traffic* (Springer, Berlin, New York 2004).
  - [4] J.-B. Lesort (editor). *Transportation and Traffic Theory*, Proceedings of the 13th International Symposium on Transportation and Traffic Theory (Elsevier Science Ltd, Oxford 1996).
  - [5] A. Ceder (editor). *Transportation and Traffic Theory*, Proceedings of the 14th International Symposium on Transportation and Traffic Theory (Elsevier Science Ltd, Oxford 1999).
  - [6] M.A.P. Taylor (editor). *Transportation and Traffic Theory in the 21st Century*, Proceedings of the 15th International Symposium on Transportation and Traffic Theory (Elsevier Science Ltd, Amsterdam 2002).
  - [7] L. Elefteriadou, R.P. Roess, W.R. McShane, *Transportation Research Record* **1484**, 80–89 (1995).
  - [8] B.N. Persaud, S. Yagar, R. Brownlee: *Transportation Research Record* **1634**, 64–69 (1998).
  - [9] M. Lorenz, L. Elefteriadou, *Transportation Research Circular* **E-C018**, 84–95 (2000).
  - [10] D. Chowdhury, L. Santen, A. Schadschneider. *Physics Reports* **329**, 199 (2000).
  - [11] D. Helbing. *Rev. Mod. Phys.* **73**, 1067–1141 (2001).
  - [12] T. Nagatani. *Rep. Prog. Phys.* **65**, 1331–1386 (2002).
  - [13] K. Nagel, P. Wagner, R. Woesler. *Operation Res.* **51**, 681–716 (2003).
  - [14] D.E. Wolf, M. Schreckenberg, A. Bachem (editors). *Traffic and Granular Flow*, Proceedings of the International Workshop on Traffic and Granular Flow, October 1995 (World Scientific, Singapore 1995).
  - [15] M. Schreckenberg, D.E. Wolf (editors). *Traffic and Granular Flow' 97*, Proceedings of the International Workshop on Traffic and Granular Flow, October 1997 (Springer, Singapore 1998).
  - [16] D. Helbing, H.J. Herrmann, M. Schreckenberg, D.E. Wolf (editors). *Traffic and Granular Flow' 99*, Proceedings of the International Workshop on Traffic and Granular Flow, October 1999, (Springer, Heidelberg 2000).
  - [17] M. Fukui, Y. Sugiyama, M. Schreckenberg, D.E. Wolf (editors). *Traffic and Granular Flow' 01*, Proceedings of the International Workshop on Traffic and Granular Flow, October 2001, (Springer, Heidelberg 2003).
  - [18] S.P. Hoogendoorn, P.H.L. Bovy, M. Schreckenberg, D.E. Wolf (editors). *Traffic and Granular Flow' 03*, Proceedings of the International Workshop on Traffic and Granular Flow, October 2003, (Springer, Heidelberg 2005) (in press).
  - [19] B.S. Kerner, P. Konhäuser, M. Schilke, *Phys. Rev. E* **51**, 6243–6246 (1995).
  - [20] D. Helbing, A. Hennecke, M. Treiber: *Phys. Rev. Lett.* **82**, 4360 (1999).
  - [21] M. Treiber, A. Hennecke, D. Helbing, *Phys. Rev. E* **62**, 1805–1824 (2000).
  - [22] H.Y. Lee, H.-W. Lee, D. Kim: *Phys. Rev. E* **59**, 5101 (1999).
  - [23] B. S. Kerner, *Phys. Rev. Lett.* **81**, 3797 (1998).
  - [24] B. S. Kerner, *Phys. Rev. E* **65**, 046138 (2002).
  - [25] B.S. Kerner, S.L. Klenov: *J. Phys. A: Math. Gen.* **35**, L31 (2002).
  - [26] B.S. Kerner, S.L. Klenov, D.E. Wolf, *J. Phys. A: Math. Gen.* **35** 9971–10013 (2002).
  - [27] B.S. Kerner, S.L. Klenov, *Phys. Rev. E* **68** 036130 (2003).
  - [28] B.S. Kerner, S.L. Klenov, *J. Phys. A: Math. Gen.* **37** 8753–8788 (2004).
  - [29] L.C. Davis, *Phys. Rev. E* **69** 016108 (2004).
  - [30] H.K. Lee, R. Barlović, M. Schreckenberg, D. Kim, *Phys. Rev. Lett.* **92**, 238702 (2004).
  - [31] R. Jiang, Q.S. Wu, *J. Phys. A: Math. Gen.* **37**, 8197–8213 (2004).
  - [32] B.S. Kerner, *Transportation Research Record* **1710**, 136 (2000).
  - [33] Concerning synchronized flow states in the vicinity of the bottleneck associated with a resulting congested pattern, we should note that assumptions used in our nucleation model are satisfied only for a localized SP (LSP) [3]. As a result, synchronized flow states at the bottleneck are drawn in Fig. 1 (b, c) and in other illustrations only for the case in which the congested pattern is an LSP.
  - [34] R. Mahnke, N. Pieret, *Phys. Rev. E* **56**, 2666 (1997).
  - [35] R. Mahnke, J. Kaupužs, *Phys. Rev. E* **59**, 117 (1999).
  - [36] R. Kühne, R. Mahnke, I. Lubashevsky, J. Kaupužs, *Phys. Rev. E* **66** 066125 (2002).
  - [37] R. Kühne, I. Lubashevsky, R. Mahnke, J. Kaupužs, *cond-mat/0405163* (2004).
  - [38] C. W. Gardiner, *Handbook of Stochastic Methods for Physics, Chemistry, and the Natural Sciences* (Springer, Berlin, 1994).
  - [39] N. G. van Kampen, *Stochastic Processes in Physics and Chemistry* (North-Holland Physics Publishing, 1984).



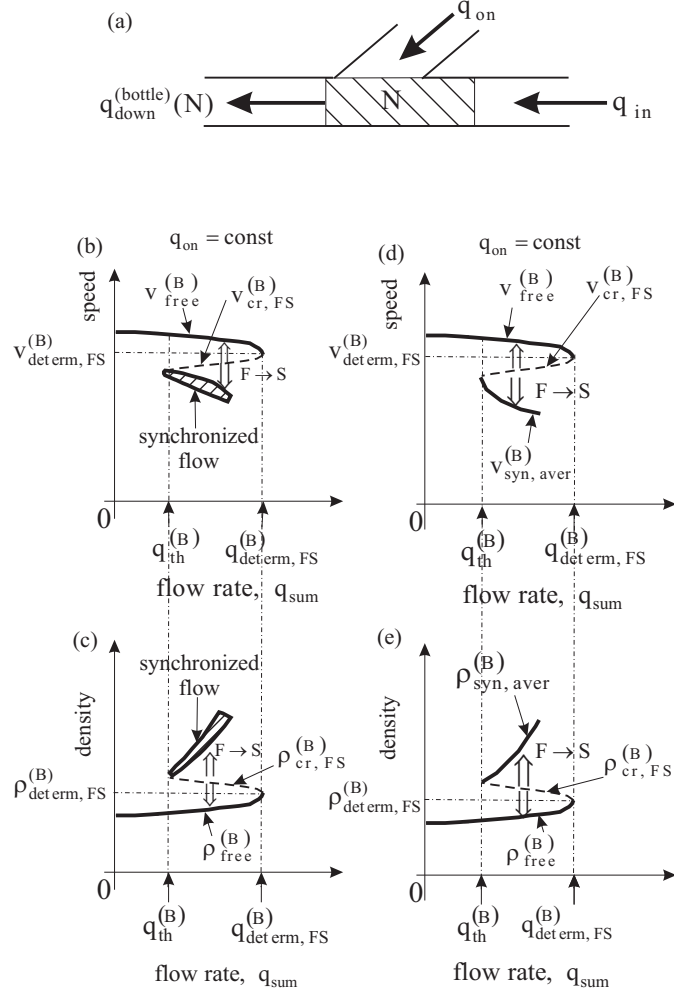


FIG. 1: Explanation of the basis of nucleation model: (a) Sketch of an on-ramp bottleneck. (b, c) – Z-shaped speed-flow (a) and the associated S-shaped density-flow characteristics for an F→S transition. (d, e) – Simplified Z-shaped speed-flow (d) and S-shaped density-flow characteristics (e) related to (b) and (c), respectively.

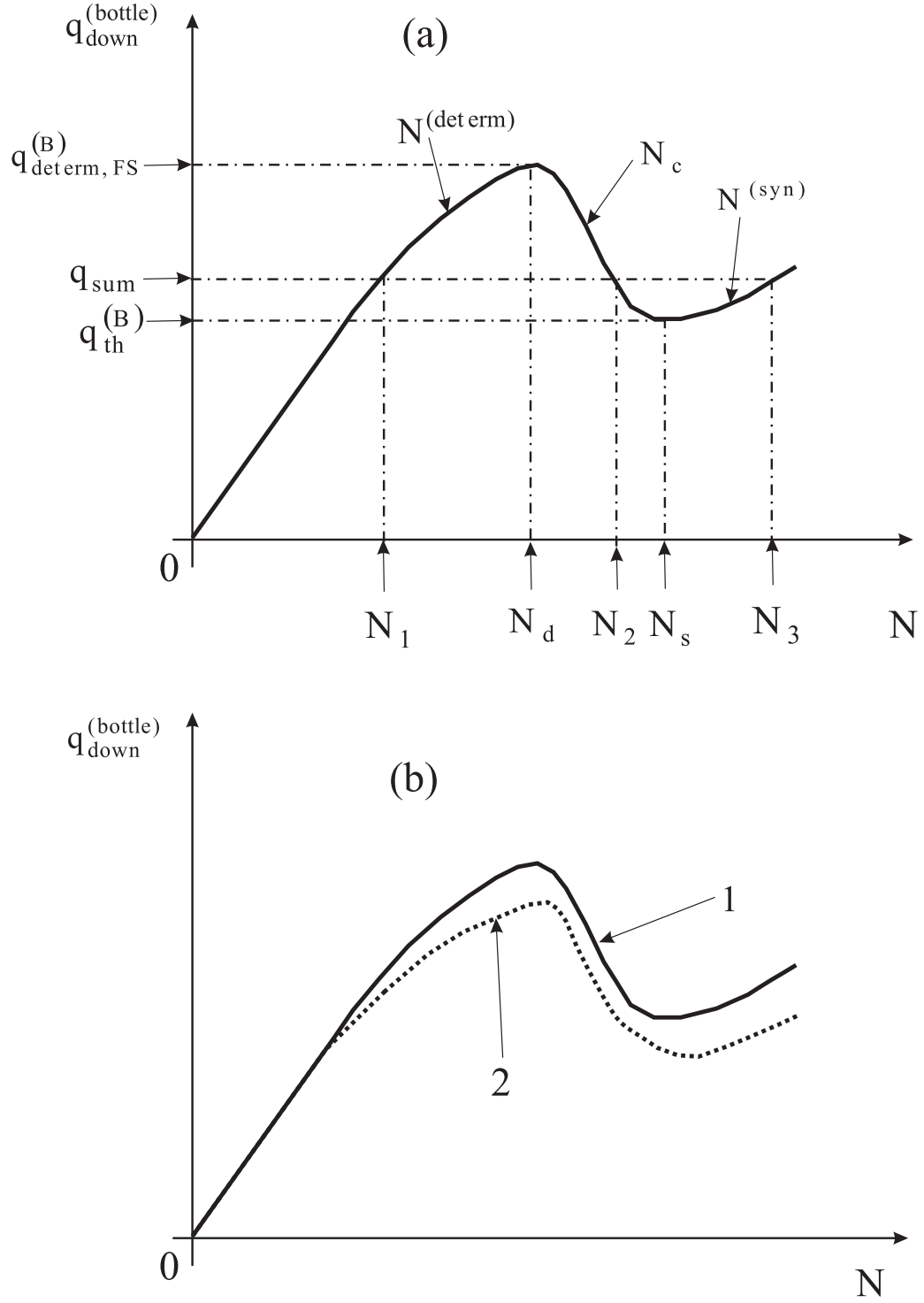


FIG. 2: Qualitative dependencies of the outflow rate  $q_{\text{down}}^{(\text{bottle})}$  on the total vehicle number  $N$  within the cluster localized at the bottleneck (a), and possible dependencies of the N-shaped function  $q_{\text{down}}^{(\text{bottle})}(N)$  on  $q_{\text{on}}$  for two different values  $q_{\text{on}}$  (b); curve 1 for  $q_{\text{on}} = q_{\text{on}}^{(1)}$ , curve 2 for  $q_{\text{on}} = q_{\text{on}}^{(2)} > q_{\text{on}}^{(1)}$ .

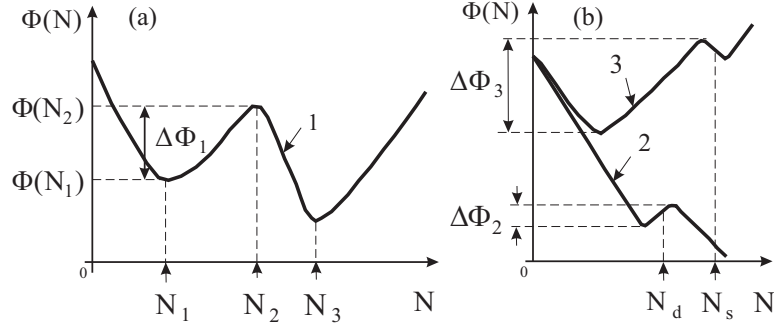


FIG. 3: Qualitative shape of the potential  $\Phi(N)$  (22) for different flow rates  $q_{\text{sum}}$ : curves 1, 2, and 3 are related to the corresponding flow rates  $q_{\text{sum}}^{(1)}$ ,  $q_{\text{sum}}^{(2)}$ , and  $q_{\text{sum}}^{(3)}$  satisfying the condition  $q_{\text{sum}}^{(3)} < q_{\text{sum}}^{(1)} < q_{\text{sum}}^{(2)}$ .

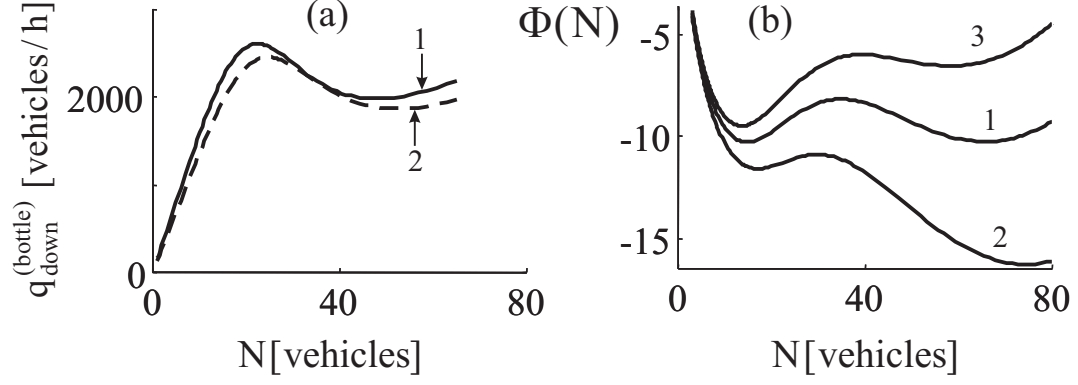


FIG. 4: N-shaped function  $q_{\text{down}}^{(\text{bottle})}(N)$  (32) (a) for  $q_{\text{on}} = 100$  vehicles/h (curve 1) and  $q_{\text{on}} = 600$  vehicles/h (curve 2), and the associated potential  $\Phi$  (22) (b) as functions of the vehicle number  $N$  for  $q_{\text{on}} = 100$  vehicles/h and for three different total flow rates  $q_{\text{sum}}$ : 2070 (curve 3), 2200 (curve 1), 2400 vehicles/h (curve 2).

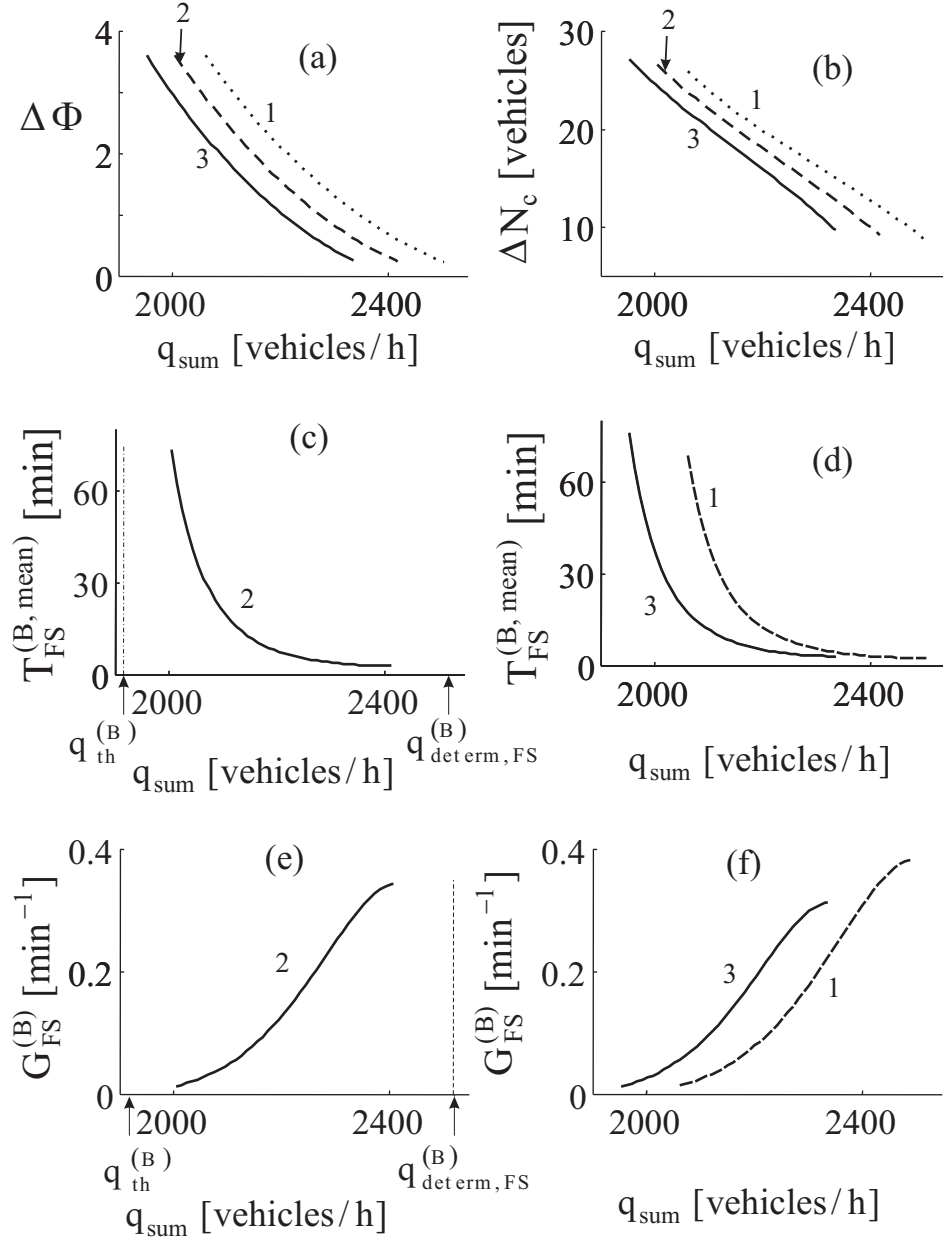


FIG. 5: Potential barrier  $\Delta\Phi$  (21) (a), critical vehicle number difference  $\Delta N_c$  (18) (b), mean time delay for speed breakdown  $T_{\text{FS}}^{(\text{B}, \text{mean})}$  (20) (c, d), and nucleation rate for speed breakdown  $G_{\text{FS}}^{(\text{B})}$  (24) (e, f) as functions of the total flow rate  $q_{\text{sum}}$  for three different flow rates  $q_{\text{on}}$ : 100 (curves 1), 300 (curves 2), 800 (curves 3) vehicles/h.

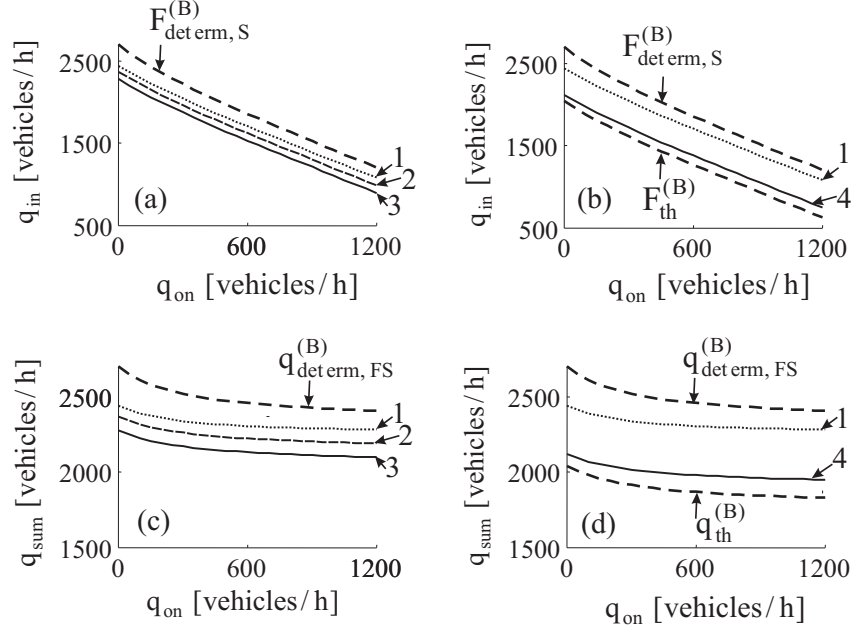


FIG. 6: Characteristics of the nucleation model: (a, b) - Boundaries of constant values of the nucleation rate  $G_{FS}^{(B)}$  of speed breakdown (curves 1–4), the critical boundary  $F_{determin, S}^{(B)}$  for deterministic speed breakdown (curves  $F_{determin, S}^{(B)}$ ), and the threshold boundary  $F_{th}^{(B)}$  (curve  $F_{th}^{(B)}$ ) as functions of the flow rates  $q_{on}$  and  $q_{in}$ . (c, d) - Dependencies of the flow rate  $q_G^{(B)}$  (34) (curves 1–4), the critical flow rate  $q_{determin, FS}^{(B)}$  (4) for deterministic speed breakdown (curves  $q_{determin, FS}^{(B)}$ ), and the threshold flow rate  $q_{th}^{(B)}$  (19) (curve  $q_{th}^{(B)}$ ) as functions of  $q_{on}$ . Curves 1–4 are related to different given values  $\zeta$  for the nucleation rate of speed breakdown  $G_{FS}^{(B)}$  in (33):  $1/3.5$  (curves 1),  $0.2$  (curves 2),  $0.1$  (curves 3),  $1/60$  (curves 4)  $\text{min}^{-1}$ . The nucleation model cannot be applied for  $q_{on} = 0$ , therefore, the points in all figures in the vicinity of  $q_{on} = 0$  show only the tendency of the boundaries in (a, b) and the flow rates in (c, d) for the limiting case of small values  $q_{on}$  in which, however, the on-ramp inflow rate  $q_{on} > 0$ , specifically, it is assumed that the deterministic cluster still exists at the bottleneck.